Pomeranchuk effect and spin-gradient cooling of Bose-Bose mixtures in an optical lattice

Yongqiang Li, M. Reza Bakhtiari, Liang He, and Walter Hofstetter

temperature, such as cooling based on extracting entropy from the region or species of interests [1, 16–19]. Recently, a cooling approach using spin-gradient adiabatic demagnetization was proposed in Ketterle's group [2], and based on it a temperature of 350 picokelvin has been achieved for a two-component Mott insulator of ^{87}Rb in a three-dimensional (3D) lattice [14, 20]. However, this temperature is still higher than the critical temperature of the magnetic phase transition [15, 21]. In addition, direct evidence for the validity of the spin-gradient cooling scheme is still lacking due to severe approximations in the theoretical discussion [1]. As far as we know, the only theoretical simulation related to the cooling of a two-component bosonic lattice gas in the presence of a magnetic field gradient has been performed by studying the domain wall dynamics of the Mott insulator via mapping it onto a spin model, where a cooling effect is also observed during adiabatic demagnetization [22].

Due to isolation of the system from the environment, entropy is more suitable than temperature for characterizing thermodynamical properties. Entropy controls quantum phase transitions since it is related to the number of accessible quantum states [1]. Therefore, a crucial issue related to cooling is how entropy is distributed in the strongly interacting many-body systems in current experiments [2, 6, 14, 19] and how the entropy redistributes during the adiabatic process of spin-gradient cooling [14]. These questions motivated our study in this paper focusing on the thermodynamical properties of two-component Bose gases in optical lattices in the presence of an external harmonic trap. While the thermodynamics of strongly interacting two-component Fermi gases has been investigated in detail [23–33] and the resulting critical entropy per particle $s \approx k_B \ln 2$ at the fermionic Mott-insulator transition has been achieved experimentally in a 3D cubic lattice [33, 34], less attention has been paid to the thermodynamics of two-component bosonic systems [35]. In Ref. [21], the critical entropy for magnetic ordering of two-component *hard-core* bosons has been investigated in a 3D homogeneous

I. INTRODUCTION

Exploring the thermodynamics of interacting many-body systems has been arguably one of the most important achievements of cold-atomic gases, whether solely trapped by an external potential or loaded into an optical lattice. A key experimental requirement is reliable thermometry, with a precision below the degeneracy point where quantum effects start to dominate. To date, the temperature of a dilute (bosonic) gas in free space has been measured by conventional time-of-flight thermometry [1] based on absorption imaging of an expanding gas released from the trap. For a wide range of experiments, this thermometric approach has been successful. However it loses its applicability when the bosons are loaded into an optical lattice, due to the reduced kinetic energy of the atoms [1, 2]. In a frequently used approximate approach, the temperature is first measured in the absence of the optical lattice, which is then ramped up gradually. One thus determines the final temperature of the gas under the assumption of ramping up the lattice adiabatically, which is a challenging task itself. Therefore the need for an alternative approach is inevitable and the search for other thermometers, directly applicable in optical lattices, has been the subject of several theoretical proposals [1].

One of the ultimate goals of experiments on cold-atomic gases in optical lattices is to include the spin degree of freedom and to simulate solid-state phenomena such as high-temperature superconductivity whose underlying mechanism is still elusive [3, 4]. Recently, bosons with a spin degree of freedom have been loaded into optical lattices [2, 5, 6] and significant efforts have been made to achieve a magnetic phase transition in the two-component bosonic system which has a rich phase diagram [7–10]. However, at present it is still challenging to observe these quantum magnetic phases in an optical lattice due to the extremely low critical temperature which is governed by second-order tunneling [11–15]. Different cooling schemes have been proposed for lowering the

system, where a critical entropy per particle of $0.35k_B$ for the XY-ferromagnetic phase and $0.5k_B$ for the Z-Néel antiferromagnetic phase have been found. Here, we will focus on the thermodynamical properties of realistic two-component bosons in a 3D cubic optical lattice *in the presence of an external trap*, and investigate the validity of spin-gradient demagnetization cooling, which is in principle capable of cooling the system down to the critical temperature of magnetic order. This system can be approximately described by a single-band Bose-Hubbard model and is investigated by bosonic dynamical mean field theory (BDMFT) [10, 36–38], both in combination with a local density approximation (LDA) and by its full real-space implementation [15].

The paper is organized as follows: in section II we give a detailed description of the model and our approach used to calculate the entropy in the inhomogeneous system. In section III we present the finite temperature phase diagram of a Bose-Bose mixture in an optical lattice. We then discuss the entropy distribution in the presence of a harmonic trap without magnetic field gradient. Finally we give a detailed discussion of the case where a magnetic field gradient is applied. We conclude in section IV.

II. MODEL AND METHOD

We consider two species of bosonic atoms [5] or, alternatively, atoms in two different hyperfine states [2, 6], in an optical lattice in the presence of an external harmonic trap. Within the tight-binding picture, this system can be described by a single-band Bose-Hubbard model:

$$\mathcal{H} = -\sum_{\substack{<i,j> \\ \nu=b,d}} t_\nu (b^\dagger_{i\nu} b_{j\nu} + h.c) + \frac{1}{2}\sum_{i,\lambda\nu} U_{\lambda\nu}\hat{n}_{i\lambda}(\hat{n}_{i\nu} - \delta_{\lambda\nu})$$
$$+ \sum_{i,\nu=b,d} (V_i - \mu_\nu)\hat{n}_{i\nu} - \sum_{i,\nu} \mu^\nu_{mag}B(x_i)\hat{n}_{i\nu} \quad (1)$$

Moreover, we consider a linear position-dependence of the magnetic field in x direction, *i.e.*, $B(x_i) = c\,x_i$ where c is the magnetic field gradient and x_i the distance from the harmonic trap center, which describes the recent experiment [14]. This leads to

$$H_B = -\sum_{i,\nu} \mu^\nu_{mag}B(x_i)\hat{n}_{i\nu} = -\sum_{i,\nu} \mu^\nu_{mag}c\,x_i\hat{n}_{i\nu}$$
$$\equiv -\sum_{i,\nu} V^\nu_{grad}x_i\hat{n}_{i\nu} \quad (2)$$

In the Hamiltonian, $\langle i,j\rangle$ denotes the summation over nearest neighbors sites and the two boson species are labelled by the index $\lambda(\nu) = b, d$. Due to different masses or a spin-dependent optical lattice, these two species generally have different hopping amplitudes t_b and t_d. The bosonic creation (annihilation) operator for species ν at site i is $b^\dagger_{i\nu}$ ($b_{i\nu}$) and the local density is $\hat{n}_{i,\nu} = b^\dagger_{i\nu}b_{i\nu}$. $U_{\lambda\nu}$ denotes the inter- and intra-species interactions, which

can be tuned via a Feshbach resonance [39] or by a spin-dependent lattice [6]. μ_ν denotes the global chemical potential for the two bosonic species and V_i is the harmonic trapping potential. μ^ν_{mag} denotes the magnetic moment of component ν and $B(x_i)$ is the magnetic field along the x axis.

Bosonic DMFT (BDMFT) has been developed [36] and implemented [10, 37, 38] to provide a non-perturbative description of zero- and finite-temperature properties of the homogeneous Bose-Hubbard model including magnetic ordering. In order to account for the external trapping potential, we have recently developed real-space BDMFT (RBDMFT), whose detailed formalism is presented in [15]. In parallel to RBDMFT, here we also employ an LDA scheme combined with single-site BDMFT to explore the system. The advantage of the latter approach is the larger system size accessible. The validity and limitations of this approach have been investigated by a quantitative comparison with the more rigorous RBDMFT method [15]. In our LDA+BDMFT calculations, the chemical potentials are adjusted locally according to the trapping potential, i.e., $\mu_\nu(r) = \mu_\nu - V_0 r^2$, where V_0 is the strength of the harmonic confinement and r is the distance from the trap center.

In general, it is difficult to calculate the entropy within BDMFT or RBDMFT directly. But assuming that the strongly interacting many-body system is in equilibrium, we can use the Maxwell relation $\frac{\partial s}{\partial \mu} = \frac{\partial n}{\partial T}$ to obtain the local entropy per site [34] at temperature T and chemical potential $\mu_s(r) = (\mu_b(r) + \mu_d(r))/2$:

$$s(\mu_s(r_0), T) = \int_{-\infty}^{\mu_s(r_0)} \frac{\partial n(r)}{\partial T}d\mu_s(r) \quad (3)$$

where $n(r) = n_b + n_d$ is the local density (*i.e.*, number of particles per lattice site) at radius r. Note that the formula (3) is only valid at fixed $\Delta\mu(r) = \mu_b(r) - \mu_d(r)$ for the two-component mixture. The density distribution obtained from BDMFT and RBDMFT is accurate enough to yield precise results for the derivative $\frac{\partial n}{\partial T}$. This relation will be used in the following to obtain the entropy distribution.

III. RESULTS

In ongoing experiments, two hyperfine states of ^{87}Rb have been loaded into optical lattices [2, 6], with interspecies and intra-species interactions in the regime $U_b \approx U_d \approx U_{bd}$. Considering the tunability of interactions via Feshbach resonances [39] or state-dependent optical lattices [6], here we choose $U_b = U_d = 1.01U_{bd}$. In the following, we investigate the finite temperature quantum phases of this system in a cubic optical lattice, as well as the temperature dependence of the entropy distribution in the presence of a harmonic trap. Finally, these thermodynamical properties are used to quantitatively describe the adiabatic spin gradient cooling scheme of [14]. In

all our calculations we consider balanced mixtures of the two components. We choose $U_{bd} = 1$ as the unit of energy, and set $k_B = 1$. z denotes the number of nearest neighbors for each lattice site. The lattice constant is set to unity.

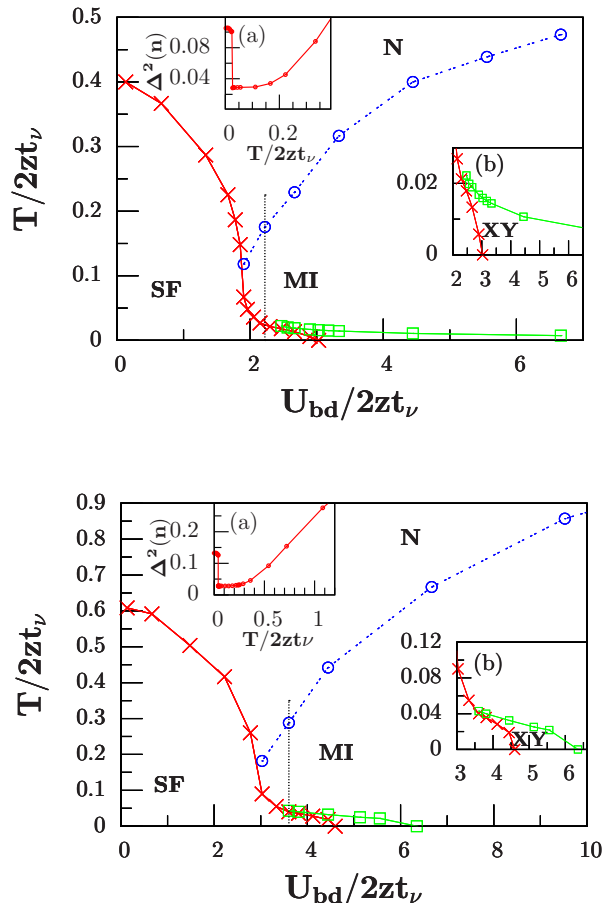## A. Pomeranchuk effect and phase diagram at finite temperature

FIG. 1: (Color online) Finite temperature phase diagram of a two-component bosonic gas in a cubic optical lattice with filling $n_b = n_d = 0.5$ (**upper**) and $n_b = n_d = 1.0$ (**lower**). The interactions are set to $U_b = U_d = 1.01 U_{bd}$, and the hopping amplitudes are $t_b = t_d$. Inset (a): fluctuations of the total density per site $n = n_b + n_d$ as a function of temperature along the vertical dotted line of the main figure. Note the reduction of local number fluctuations by heating, analogous to the *Pomeranchuk effect*. Inset (b): zoom of the main figure around the critical point of magnetic order.

In this section, we explore the finite-temperature phase diagram of two-component bosons in a homogeneous and infinite optical lattice. For strongly interacting two-component Fermi gases, the critical parameters such as the critical temperature and entropy for the transition

to a superfluid state have been determined experimentally [23] by considering entropy versus energy. For one-component bosonic gases in an optical lattice, the finite-temperature phase diagram has been studied experimentally in combination with Monte Carlo simulations [40]. However, for two-component bosonic gases, the critical behavior of the superfluid-normal phase transition has not been determined yet. In our previous work [15], phase diagrams at filling $n = 1$ and $n = 2$ for zero and fixed finite temperature have been determined for the cubic lattice. But there we mainly focused on the emergence of long-range magnetic order, which is governed by second-order tunneling and only develops at very low temperatures of the order of 100 pK. On the contrary, here we will investigate quantum criticality of the system at higher temperatures. We choose interactions $U_b = U_d = 1.01 U_{bd}$ and hopping amplitudes $t_b = t_d$. Fig. 1 shows the phase diagram of a Bose-Bose mixture in a cubic optical lattice with filling $n_b = n_d = 0.5$ (upper) and $n_b = n_d = 1$ (lower). We observe four different phases. When the interaction is weak, the atoms are delocalized and at low temperature the system is in the superfluid phase (SF), characterized by a finite value of the superfluid order parameter $\phi_\nu \equiv \langle b_\nu \rangle$. When the temperature is increased, thermal fluctuations destroy the coherence between atoms and the system goes through a phase transition into the normal phase (N). For sufficiently strong interactions, the atoms are localized and hopping processes are strongly suppressed. The system is in the XY-ferromagnetic phase (characterized by $\langle bd^\dagger \rangle > 0$ and $\phi_\nu = \langle b_\nu \rangle = 0$) at low temperature, with magnetic long-range order governed by second-order tunneling processes. Since the corresponding energy scale is very small, even weak thermal fluctuations can destroy the long-range magnetic order, and the system will go through a phase transition into a Mott insulator (MI) without order. Upon further increase of temperature, the Mott insulator melts into a normal phase which is characterized by large density fluctuations $\Delta^2(n) = \langle (n - \langle n \rangle)^2 \rangle$ where the n is the total density per site. Compared to the single-component system in a cubic optical lattice, new features of two-component bosons appear at low temperature. Near the critical interaction strength of the zero-temperature MI-SF transition, with increasing temperature, the system will first go through a phase transition from superfluid to Mott-insulator, and then cross over to the normal phase. This is because upon heating at low temperature, the system favors localization - analogous to the Pomeranchuk effect in liquid ^{3}He [31, 41] - since the Mott insulating phase of spinful bosons carries more entropy in the spin degree of freedom than the superfluid. Interestingly, the first-order phase transition from superfluid to Mott-insulator occurs at a higher temperature for filling $n = 2$ (lower plot in Fig. 1) compared to $n = 1$, indicating that it is easier to observe the Pomeranchuk effect discussed above for higher filling. Note that the XY-ferromagnetic phase at filling $n = 2$ only extends up to a finite maximum value of $U_{bd}/2zt_\nu$, which is consis-

tent with our previous work [15].

B. Entropy distribution in the trapped system with $B = 0$

In the former section, we have studied the homogeneous system and mapped out the finite-temperature phase diagram. We will now study the thermodynamics of Bose-Bose mixtures in an optical lattice in the presence of a harmonic trap. More specifically, we investigate the temperature dependence of the entropy distribution, motivated by recent experiments [2, 5, 6]. Comparison between RBMDFT and BDMFT+LDA calculations has been made to check the validity of LDA for determining the entropy. Only the results of BDMFT+LDA are given here for the 3D case in a $51 \times 51 \times 51$ cubic lattice. Throughout this section, the interactions are set to $U_b = U_d = 1.01U_{bd}$ with a harmonic trap strength $V_0 = 0.005U_{bd}$ and a total filling $n = 2$ at the trap center.

In the upper panel of Fig. 2 at high temperatures $T/U_{bd} = 0.105$, 0.11 and 0.115 (corresponding to the normal phase in Fig. 1), the Mott-insulator plateaux melt into a normal phase with entropy per site $s > \ln 3$ around the center of the harmonic trap and $s > \ln 2$ at the second Mott-insulating ring. Naturally, we can also identify the melting of the Mott insulator into the normal phase from the density profile, i.e., the corresponding Mott-plateaux at filling $n = 2$ and $n = 1$ have disappeared at this temperature. Due to the insensitivity of the density profile to a small variation of temperature, only a single density profile at temperature $T/U_{bd} = 0.11$ is shown here. There are also two peaks of the entropy density in the normal shells surrounding the Mott-insulating regions. Our simulations indicate that the transfer of entropy from superfluid to Mott insulator due to the Pomeranchuk effect does not occur in this high temperature region, since here the local entropy per particle in the superfluid is higher than in the Mott-insulator. We observe that the local entropy per particle is reduced when the temperature decreases, as shown in the lower panel of Fig. 2 at low temperatures of $T/U_{bd} = 0.035$, 0.04 and 0.045 (corresponding to the Mott insulator region in Fig. 1). Here the system has a Mott-insulator core with filling $n = 2$ in the trap center and also a Mott-insulating shell with filling $n = 1$. Correspondingly, the local entropy per site of the Mott-insulator region is $s \approx \ln 3$ in the filling $n = 2$ region and $s \approx \ln 2$ in the $n = 1$ region, respectively, since there are three possible local spin states $|\uparrow\uparrow\rangle$, $|\downarrow\downarrow\rangle$ and $|\uparrow\downarrow\rangle$ for $n = 2$, and two possible spin states $|\uparrow\rangle$, $|\downarrow\rangle$ for $n = 1$, where $\uparrow$ and $\downarrow$ denote the two bosonic species. Between the two Mott-insulating regions, there is also a superfluid shell with non-zero value of the superfluid order parameter. Interestingly, we observe a sudden drop of the entropy density around the peak of the superfluid order parameter, which indicates a fine structure in the density distribution of the phases with non-integer filling
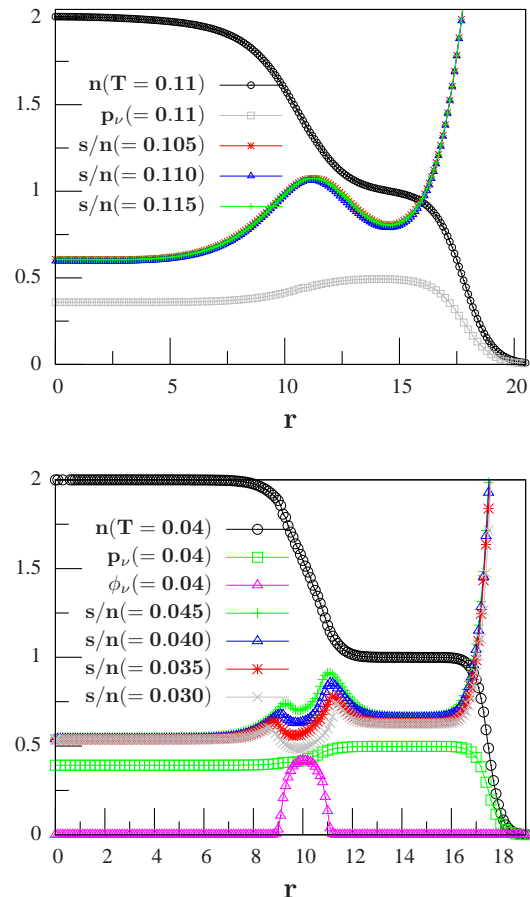

FIG. 2: (Color online) Radial profile for the total density per site ($n \equiv n_b + n_d$), parity (p_ν), local entropy per particle (s/n), and superfluid order parameter (ϕ_ν) in a 3D cubic lattice obtained by BDMFT+LDA at different temperatures. The interactions are set to $U_b = U_d = 1.01U_{bd}$, with hopping amplitudes $2zt_b = 2zt_d = 0.195U_{bd}$ and harmonic trap strength $V_0 = 0.005U_{bd}$. The unit of temperature is U_{bd}.

(superfluid and normal phase). A similar structure is also found for a one-component Bose gas in an optical lattice plus external harmonic trap [42]. Physically, the sudden change of entropy in the superfluid region is caused by the reduced number of many-body states of the system due to the formation of a condensate. It is expected that, if the temperature is lowered further, another superfluid domain forms in the region with filling $n < 1$. We have also shown the parity profile $p_\nu = \langle(1 - e^{i\pi\hat{n}_\nu})/2\rangle$ for the individual components in Fig. 2, which can be directly measured experimentally [43, 44]. Interestingly, the local parity for the individual components in the Mott-insulating region with total filling $n = 2$ is finite.

In addition, we now observe (lower plot of Fig. 2) that the local entropy per particle in the first superfluid ring is smaller in some regions than that in the Mott insulator, which indicates that a transfer of entropy from superfluid to Mott insulator can lower the temperature of the

system in this regime, which is consistent with the phase diagram for the homogeneous system in Fig. 1. This interaction-induced cooling mechanism (Pomeranchuk effect) of two-component bosonic gases in an optical lattice is expected to be visible experimentally [2, 5, 6], after further lowering the temperature. For example, in the experiment this effect could be observed via ramping up the optical lattice, where the temperature should be decreased beyond single-particle adiabatic cooling due to the Pomeranchuk effect, since the Mott-insulating region increases.
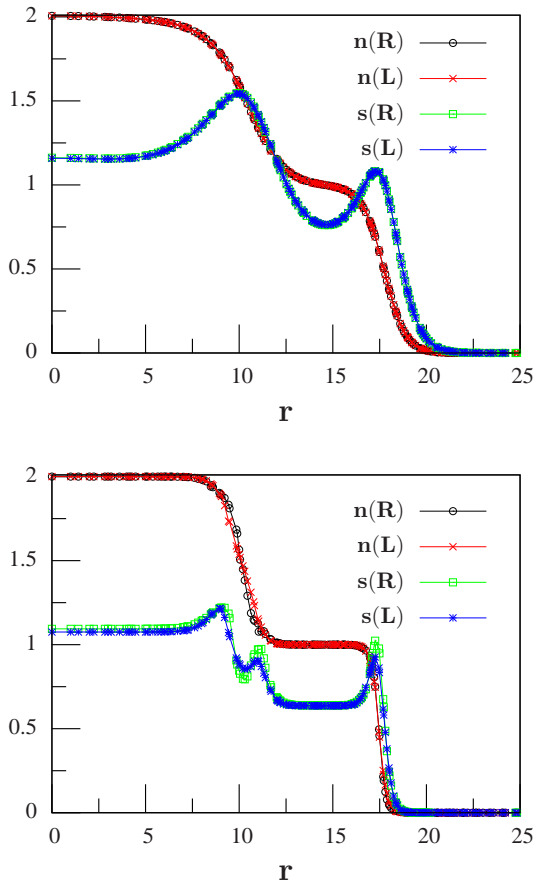

FIG. 3: (Color online) Validity of BDMFT+LDA benchmarked against RBDMFT. Density profile n_{tot} and entropy distribution s along the radial direction r at temperature $T = 0.1U_{bd}$ (**upper**) and $T = 0.03U_{bd}$ (**lower**) obtained by RBDMFT (R) and BDMFT+LDA (L) for 2D case. The interactions are set to $U_b = U_d = 1.01U_{bd}$ and the hopping amplitudes are $2zt_b = 2zt_d = 0.175U_{bd}$ with harmonic trap $V_0 = 0.005U_{bd}$.

To check the validity of BDMFT+LDA around quantum degeneracy, we investigate the density and entropy distribution for the 2D case and test the accuracy of BDMFT+LDA against RBDMFT, as shown in Fig. 3. We find excellent agreement deep inside each phase, while RBDMFT provides the slightly more accurate description of the transition region. We therefore expect that

BDMFT+LDA will also give quantitatively reliable results for the 3D case.

C. Adiabatic cooling via entropy redistribution for $B \neq 0$

We have so far investigated thermodynamical properties for equal filling of the two components. In this section, we will now study a scenario with the two species separated by a magnetic field with constant gradient which can be used experimentally to cool the system. Specifically, we simulate the adiabatic process of the spin-gradient cooling scheme proposed by Weld *et. al.* [2]. To this end, we calculate the entropy distribution of the inhomogeneous system in the presence of the field gradient, and the dependence of the entropy per particle on temperature. To simplify the calculation, we assume that the two components of the bosonic mixture have the same absolute value of the magnetic moment.

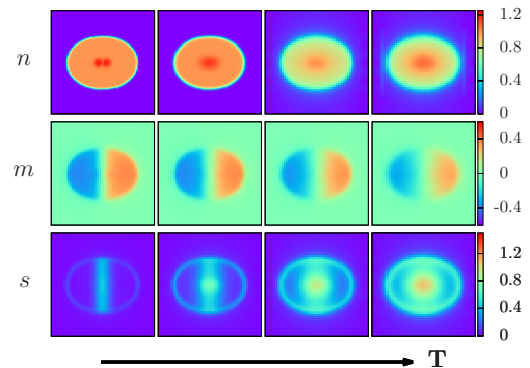### 1. Entropy distribution in the presence of field gradient

FIG. 4: (Color online) Real-space profile (here in the x-y plane of the lattice) for the local density n, magnetization m and entropy s along the $z = 0$ plane of a 3D cubic lattice using BDMFT+LDA. From left to right, the temperatures are $T/U_{bd} = 0.020$, 0.040, 0.070 and 0.095, respectively. The interactions are set to $U_b = U_d = 1.01U_{bd}$ and the hopping amplitudes are $2zt_b = 2zt_d = 0.12U_{bd}$, with total particle number $N_{tot} \approx 17000$ in a harmonic trap $V_0 = 0.004U_{bd}$ and magnetic field gradient $V_{gra} = 0.01U_{bd}$.

The two-component bosonic mixture can be separated to opposite sides of the trap by the magnetic field. At zero temperature, the two components are completely separated and a sharp domain wall forms in the trap center. At finite temperature, spin excitations, such as a pair of opposite-spin atoms swapping positions via second-order tunneling, will broaden the width of the domain wall (the width is defined as the distance from the trap center to the position where the magnetization is half

of the maximum value). As pointed out in [2, 22] the width of the domain wall depends in a simple way on the field gradient and can be used as a thermometer in the zero-tunneling limit. Fig. 4 shows the distribution of local density n, magnetization $m = (n_b - n_d)/2$, and entropy s in the $z = 0$ plane. Since the density and magnetization distributions depend on the temperature, they can be used for thermometry via in-situ measurements with single-site resolution [43, 44]. In particular, the magnetization distribution can be used as a thermometer at low temperatures down to the critical temperature of magnetic phases. From the middle row of Fig. 4 we observe that the narrow mixed region of the two components broadens with increasing temperature, which is consistent with measurements where temperatures as low as 350 pK have been measured [2, 14]. The bottom row of Fig. 4 shows the entropy distribution. The entropy is mainly carried by the spin degree of freedom of particles around the trap center, and also by delocalized particles near the edge of trap. When the temperature is lowered, the delocalized particles form a condensate. As a result, the entropy drops quickly as a function of temperature in the superfluid ring. On the other hand, the spin degree of freedom in the mixed region can still carry a large amount of entropy, even at low temperature where the entropy of the single-component superfluid becomes very small. Therefore, if one prepares the system in a state where entropy is mainly carried by a single species (*i.e.* if one initially separates the two species by a field gradient) and then transfers the entropy from the single species to the spin degree of freedom, the temperature of the system can be lowered dramatically.
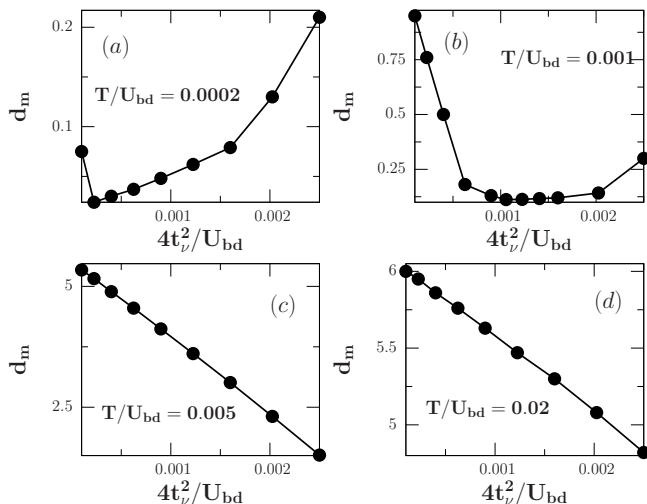

FIG. 5: Domain-wall width d_m (in units of the lattice constant) as a function of superexchange coupling at different temperatures. The width is defined as the distance from the trap center to the position where the magnetization is half of the maximum value. The interactions are set to $U_b = U_d = 1.01U_{bd}$ in a harmonic trap $V_0 = 0.004U_{bd}$ and a magnetic field gradient $V_{gra} = 0.0005U_{bd}$.

The domain-wall width can also be used as a tool to measure the strength of the resulting superexchange interactions between the atoms. As shown in panel (a) and (b) in Fig. 5, when superexchange interactions dominate over thermal fluctuations ($4t_\nu^2/U_{bd} > T$), we observe a linear dependence of the domain-wall width on the strength of the superexchange in the Mott-insulating regime. We also observe that the domain-wall width increases faster at larger hopping parameters, since in that case the mixed region is in the superfluid regime and the first-order tunneling dominates. When thermal fluctuations dominate ($4t_\nu^2/U_{bd} < T$), as shown in panels (a), (b), (c) and (d), the increase of the superexchange decreases the width of the domain wall due to minimizing the energy of the spin-spin coupling. If the temperature is increased, the minimum of the domain-wall width is shifted to higher hopping amplitudes, as shown in panels (a) and (b) in Fig. 5. We also observe that the linear dependence [2, 22] of the domain-wall width d_m only holds for temperature above the critical values T_c for magnetic ordering (see Fig. 6). The change of slope at T_c is a clear indication of the phase transition.
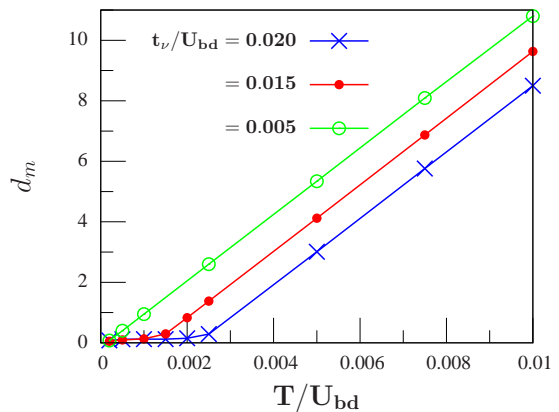

FIG. 6: (Color online) Domain-wall width d_m (in units of the lattice constant) as a function of temperature at different hopping amplitudes. The width is defined as the distance from the trap center to the position where the magnetization is half of the maximum value. The interactions are set to $U_b = U_d = 1.01U_{bd}$ in a harmonic trap $V_0 = 0.004U_{bd}$ and a magnetic field gradient $V_{gra} = 0.0005U_{bd}$.

2. Entropy per particle versus temperature

We now focus on the relation of entropy versus temperature, which gives insight how adiabatic changes affect the temperature of the system. Fig. 7 shows the entropy-temperature curve for strongly interacting two-component bosons in an optical lattice in the presence of the magnetic field, where the dashed lines are obtained by the zero-tunneling approximation [20]. Due to the deep optical lattice, our results obtained by BDMFT+LDA are in good agreement with the approximate analytical
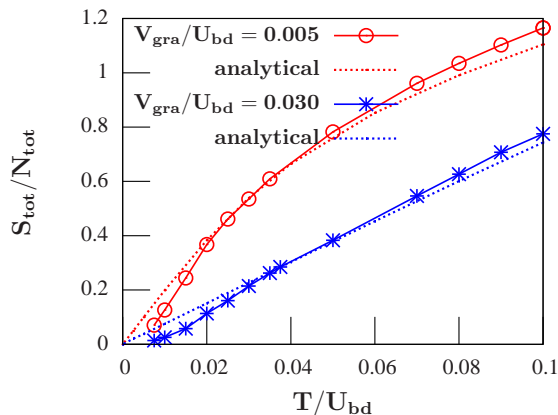
FIG. 7: (Color online) Entropy per particle versus temperature in a cubic optical lattice obtained by BDMFT+LDA, compared with the analytical zero-tunneling approximation [20]. The interactions are set to $U_b = U_d = 1.01U_{bd}$ and the hopping amplitudes to $2zt_b = 2zt_d = 0.12U_{bd}$, with total particle number $N_{tot} \approx 17000$ in a harmonic trap of strength $V_0 = 0.004U_{bd}$.

results except at low and high temperatures. At high temperature, thermal fluctuations will induce hopping of atoms. This effect is neglected in the zero-tunneling approximation, which therefore gives a lower prediction for the entropy. At low temperature, on the other hand, the entropy of the motional degree of freedom drops quickly due to condensate formation in the superfluid regime. This effect is neglected as well in the zero-tunneling approximation, which therefore gives a larger prediction for the entropy. We note that quantum Monte Carlo simulations [21] also reveal the inadequacy of the zero-tunneling approximation in the low temperature regime.

3. Adiabatic cooling via spin-gradient demagnetization

The spin-gradient cooling scheme relies on the inhomogeneous entropy distribution of the system. The main effect of the demagnetization process is to decrease the local entropy per particle in the spin-mixed regions, which is essential for long-range spin order. There are three different regions corresponding to different phases of the system, namely the superfluid, spin-mixed and one-component Mott-insulating region. Initially, the superfluid and spin-mixed region carry almost all the entropy of the system, while the entropy in the one-component Mott insulator is close to zero. When the magnetic field gradient is decreased, the spin-mixed region expands, while the one-component Mott-insulating region shrinks, and the average entropy per particle in the spin mixed region is decreased. At the same time, the temperature drops, since entropy carried by hot mobile particles is drained into the expanding mixed region with a drop of local entropy per particle. Here, we will quantita-
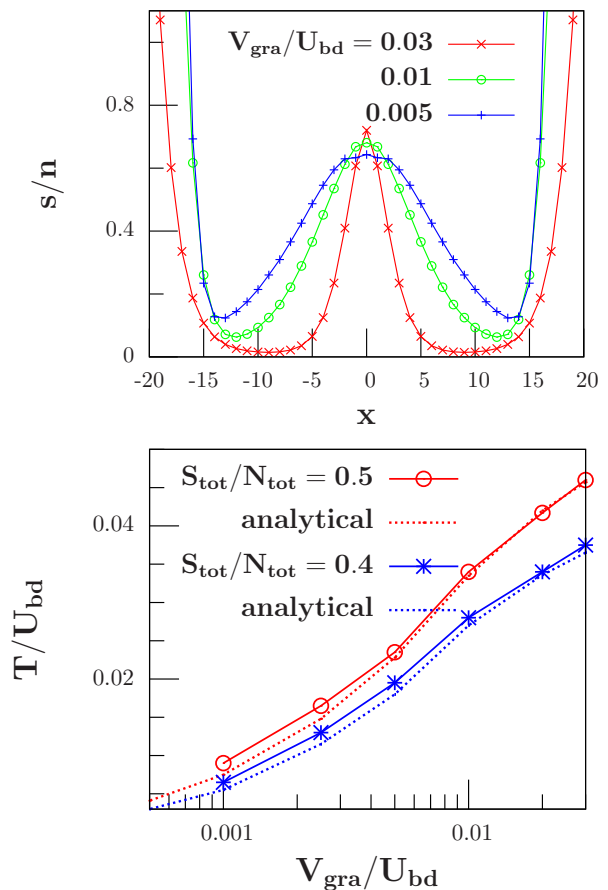

FIG. 8: (Color online) **Upper**: Field-gradient dependence of the local entropy per particle along the x direction on the $y, z = 0$ axis, for an entropy per particle $S_{tot}/N_{tot} = 0.7$. The red, green and blue lines correspond to field gradients of $V_{gra}/U_{bd} = 0.03$, 0.01 and 0.005, respectively. **Lower**: Adiabatic cooling due to spin-gradient demagnetization in a cubic lattice. Data are obtained by BDMFT+LDA and compared to the analytical zero-tunneling approximation [20]. Interactions are set to $U_b = U_d = 1.01U_{bd}$, and the hopping amplitudes are $2zt_b = 2zt_d = 0.12U_{bd}$ for total particle number $N_{tot} \approx 17000$ in a harmonic trap $V_0 = 0.0025U_{bd}$.

tively establish this scenario by considering the spatial entropy distribution and entropy-temperature relation. In the upper panel of Fig. 8, the local entropy per particle s/n is shown at different field gradient strengths for fixed total particle number and entropy. We observe that s/n decreases in the central region as the field gradient is adiabatically decreased. Since the number of spin excitations (with respect to the ferromagnet at zero temperature and in the presence of the field gradient) due to exchange of $|\uparrow\rangle$ and $|\downarrow\rangle$ particles between neighboring sites is increased in the demagnetization process, the total energy of the system decreases as well and, as a result, the temperature drops from $T/U_{bd} = 0.065$ to 0.035 when the field gradient adiabatically decreases from $V_{gra}/U_{bd} = 0.03$ to 0.005. The resulting cooling efficiency is shown in the lower panel of Fig. 8. The demagneti-

zation cooling curve obtained via BDMFT simulations is in good agreement with results from the zero-tunneling limit [20], since here we choose the optical lattice relatively deep which makes t_ν/U_{bd} very small. In addition, the demagnetization cooling appears to be less efficient at larger magnetic field gradients. This is because the strong field gradient repels particles to the outer regions of the trap, which makes the trap center superfluid with enhanced entropy compared to the Mott insulator. This effect reduces the entropy capacity of the spin degree of freedom at high field gradients.

IV. CONCLUSION

In conclusion, we have investigated the thermodynamics of a two-component Bose gas loaded into an optical lattice in the presence of an external trap, using BDMFT+LDA and the newly developed real-space BDMFT. We obtain the finite-temperature phase diagram and find that at low temperature, remarkably, the

system can be *heated* into a Mott insulator, analogous to the Pomeranchuk effect in ^{3}He. By investigating the entropy redistribution of the system during adiabatic spin-gradient demagnetization, we observe efficient cooling due to entropy transfer from the single species domains to the mixed region, and provide a quantitative theoretical validation of recent experiments [2, 14]. We expect our work to provide valuable insight for realizing quantum magnetic phases in upcoming experiments.

[1] D. C. McKay and B. DeMarco, Rep. Prog. Phys. **74**, 054401 (2011).

[2] D. M. Weld, P. Medley, H. Miyake, D. Hucul, D. E. Pritchard, and W. Ketterle, Phys. Rev. Lett. **103**, 245301 (2009).

[3] W. Hofstetter, J. I. Cirac, P. Zoller, E. Demler, and M. D. Lukin, Phys. Rev. Lett. **89**, 220407 (2002).

[4] T. Esslinger, Condensed Matter Physics **1**, 129 (2010).

[5] J. Catani, L. De Sarlo, G. Barontini, F. Minardi, and M. Inguscio, A **77**, 011603 (2008).

[6] B. Gadway, D. Pertot, R. Reimann, and D. Schneble, Phys. Rev. Lett. **105**, 045303 (2009).

[7] L.-M. Duan, E. Demler, and M. D. Lukin, Phys. Rev. Lett. **91**, 090402 (2003).

[8] E. Altman, W. Hofstetter, E. Demler, and M. Lukin, New Jounal of Physics **5**, 113 (2003).

[9] Ş. G. Söyler, B. Capogrosso-Sansone, N. V. Prokof'ev, and B. V. Svistunov, New J. Phys. **11**, 073036 (2009).

[10] A. Hubener, M. Snoek, and W. Hofstetter, Phys. Rev. B **80**, 245109 (2009).

[11] A. Auerbach, *Interacting electrons and quantum magnetism*, (Springer-Verlag, New York, 1994).

[12] S. Fölling, S. Trotzky, P. Cheinet, M. Feld, R. Saers, A. Widera, T. Müller, and I. Bloch, Nature (London) **448**, 1029 (2007).

[13] S. Trotzky, P. Cheinet, S. Fölling, M. Feld, U. Schnorrberger, A. M. Rey, A. Polkovnikov, E. A. Demler, M. D. Lukin, and I. Bloch, Science **319**, 295 (2008).

[14] P. Medley, D. M. Weld, H. Miyake, D. E. Pritchard, and W. Ketterle, Phys. Rev. Lett. **106**, 195301 (2011).

[15] Y.-Q. Li, M. R. Bakhtiari, L. He, and W. Hofstetter, Phys. Rev. B **84**, 144411 (2011).

[16] M. Popp, J.-J. Garcia-Ripoll, K. G. Vollbrecht, and J. I. Cirac, Phys, Rev. A **74**, 013622 (2006).

[17] T. Ho and Q. Zhou, Natl. Acad. Sci. U.S.A **106**, 6919 (2009).

[18] T. Ho and Q. Zhou, arXiv:0911.5506.

[19] J. Catani, G. Barontini, G. Lamporesi, F. Rabatti, G. Thalhammer, F. Minardi, S. Stringari, and M. Inguscio, Phys. Rev. Lett. **103**, 140401 (2009).

[20] D. M. Weld, H. Miyake, P. Medley, D. E. Pritchard, and W. Ketterle, Phys. Rev. A **82**, 051603 (2010).

[21] B. Capogrosso-Sansone, Ş. G. Söyler, N. V. Prokof'ev, and B. V. Svistunov, Phys. Rev. A **81**, 053622 (2010).

[22] S. S. Natu and E. J. Mueller, Phys. Rev. A **82**, 013612 (2010).

[23] L. Luo, B. Clancy, J. Joseph, J. Kinast, and J. E. Thomas, Phys. Rev. Lett. **98**, 080402 (2007).

[24] A. Bulgac, J. E. Drut, and P. Magierski, Phys. Rev. Lett. **99**, 120401 (2007).

[25] G. B. Partridge, W. Li, R. I. Kamar, Y. Liao, and R. G. Hulet, Science **311**, 503 (2006).

[26] J. T. Stewart, J. P. Gaebler, C. A. Regal, and D. S. Jin, Phys. Rev. Lett **97**, 220406 (2006).

[27] H. Hu, P. D. Drummond, and X. Liu, Nature Physics **3**, 469 (2007).

[28] S. Nascimbène, N. Navon, K. J. Jiang, F. Chevy, and C. Salomon, Nature (London) **463**, 1057 (2010).

[29] N. Navon, S. Nascimbène, F. Chevy, and C. Salomon, Science **328**, 729 (2010).

[30] M. Horikoshi, S. Nakajima, Masahito Ueda, and T. Mukaiyama, Science **327**, 442 (2010).

[31] F. Werner, O. Parcollet A. Georges, and S. R. Hassan, Phys. Rev. Lett. **95**, 056401 (2005).

[32] T. Paiva, R. Scalettar, M. Randeria, and N. Trivedi, Phys. Rev. Lett. **104**, 066406 (2010).

[33] R. Jördens, L. Tarruell, D. Greif, T. Uehlinger, N. Strohmaier, H. Moritz, T. Esslinger, L. De Leo, C. Kollath, A. Georges, V. Scarola, L. Pollet, E. Burovski, E. Kozik, and M. Troyer, Phys. Rev. Lett. **104**, 180401 (2010).

[34] U. Schneider, L. Hackermüller, S. Will, Th. Best, I.

Bloch, T. A. Costi, R. W. Helmes, D. Rasch, and A. Rosch, Science **322**, 1520 (2008).

[35] S. Guertler, M. Troyer, and F. Zhang, Phys. Rev. B **77**, 184505 (2008).

[36] K. Byczuk and D. Vollhardt, Phys. Rev. B **77**, 235106 (2008).

[37] W. Hu and N. Tong, Phys. Rev. B **80**, 245110 (2009).

[38] P. Anders, E. Gull, L. Pollet, M. Troyer, and P. Werner, Phys. Rev. Lett. **105**, 096402 (2010).

[39] A. Widera, O. Mandel, M. Greiner, S. Kreim, T. W. Hänsch, and I. Bloch, Phys. Rev. Lett. **92**, 160406 (2004).

[40] S. Trotzky, L. Pollet, F. Gerbier, U. Schnorrberger, I. Bloch, N. V. Prokof'ev, B. Svistunov, and M. Troyer, Nature Physics **10**, 1799 (2010).

[41] R. C. Richardson, Rev. Mod. Phys. **69**, 683 (1997).

[42] T. Ho and Q. Zhou, Phys. Rev. Lett. **99**, 120404 (2007).

[43] W. S. Bakr, J. I. Gillen, A. Peng, S. Fölling, and M. Greiner, Nature **462**, 74 (2009).

[44] J. F. Sherson, C. Weitenberg, M. Endres, M. Cheneau, I. Bloch, and S. Kuhr, Nature **467**, 68 (2010).